



An Autonomous and Controllable Light-Driven DNA Walking Device**

Mingxu You, Yan Chen, Xiaobing Zhang,* Haipeng Liu, Ruowen Wang, Kelong Wang, Kathryn R. Williams, and Weihong Tan*

The development of nanotechnology has been largely inspired by the biological world. The complex, but well-organized, living system hosts an array of molecular-sized machines responsible for information processing, structure building and, sometimes, movement. Molecular motors are tiny protein machines that power motion in the cellular world, for example, myosins moving on actin filaments and dyneins or kinesins walking along microtubule tracks.^[1]

Artificial DNA-based motors have recently emerged to mimic molecular motors^[2] and to perform tasks in cargo transport^[2c] and biosynthesis.^[2f] The programmable assembly and simplicity of polynucleotide interactions have made DNAs suitable for the control of progressive and directional movement at the molecular level. However, energy supply is a major concern for any motor.^[3] Biological molecular motors employ free energy based on the binding and hydrolysis of ATP, whereas artificial DNA walkers have previously explored energy supplied by DNA hybridization^[4] or hydrolysis of either the DNA/RNA backbone^[5] or ATP molecules.^[6] These artificial walking devices are still in their infancy, and they are not as powerful as their protein counterparts from nature. Still, identification of new types of energy supplies could play a major role in the development of the next-generation mechanical robots.

Biological motors normally operate in a constant environment without external intervention, and they remain in operation as long as a source of energy is available. Thus,

these biological motors are considered to be autonomous. For artificial DNA walkers, however, nonautonomous locomotion by regular addition of fuel^[7] is always much simpler from a design standpoint, compared to an autonomous device. On the other hand, the capability of autonomous motion sometimes results in decreased controllability^[2,5,6] because the device cannot be stopped at a desired position or time, or once stopped, it cannot be easily restarted. Therefore, construction of free-running and autonomous “true” molecular motors,^[2b] in comparison to nonautonomous designs, is still essential to the operation of nanomachines that mimic biological function. The availability of such an easily controllable, free-running DNA walker would also be significant for the future design of nanorobots to perform multiple and complex functions.

We report here a new light energy-powered DNA walker capable of regulated autonomous movement along a nucleic acid track. It has been widely known that photochemical energy sources can serve as inputs for molecular-level switches in the operation of nanomachines.^[8] We recently found that aromatic hydrocarbons (e.g., pyrene molecules) can efficiently facilitate the photolysis of disulfide bonds within artificial nucleic acid backbones^[9] and that a catalytic cleavage function could be achieved through the design of pyrene-incorporated DNAzyme analogues (Figure 1a). This same pyrene-assisted photolysis reaction is also a major component of our DNA walker design (Figure 1b).


Photon radiation, which is virtually unlimited, supplies the energy (together with DNA hybridization free energy) for this type of nanomachine, and the amount of energy input to operate such machines can be readily controlled by using different intensities of excitation light. Moreover, by taking advantage of recent developments in laser and near-field techniques, high spatial and temporal resolution can be achieved from light control as well.^[10] With its renewable energy supply, we envision that the light-powered DNA walker will allow us to precisely control the speed and motion of nanorobots and, hence, advance the progress of molecular biology in the future. This work represents the first light-powered DNA walking devices able to achieve controllable, autonomous, and directional movement, and it expands the scope of energy supplies available to power nanosized motion.

The walking system consists of three parts: a single-stranded DNA track (**T**), four anchorage sites (**S1**, **S2**, **S3**, and **S4**), and a light-sensitive walker (**W**, Figure 1). Similar to previous design of processive walker by He et al.,^[2f,5a] the track contains four 21-nucleotide binding regions that are complementary to the recognition tag of the respective

[*] M. You, Dr. Y. Chen, Dr. H. Liu, Dr. R. Wang, Dr. K. Wang, Dr. K. R. Williams, Prof. Dr. W. Tan
Department of Chemistry and Physiology and Functional Genomics
Center for Research at the Bio/Nano Interface
Shands Cancer Center, UF Genetics Institute
and McKnight Brain Institute, University of Florida
Gainesville, FL 32611-7200 (USA)
E-mail: tan@chem.ufl.edu

Prof. Dr. X. Zhang, Prof. Dr. W. Tan
State Key Laboratory for Chemo/Biosensing and Chemometrics
College of Biology and College of Chemistry and Chemical
Engineering
Hunan University, Changsha 410082 (P.R. China)
E-mail: xiaobingzhang89@hotmail.com

[**] The authors would like to thank the Interdisciplinary Center for Biotechnology Research (ICBR) at the University of Florida for technical support. This work is supported by grants awarded by the National Institutes of Health (grant numbers GM066137, GM079359, and CA133086) and by the NSF. This work was also supported by the National Key Scientific Program of China (2011CB911001, 2011CB911003).

 Supporting information for this article is available on the WWW under <http://dx.doi.org/10.1002/anie.201107733>.

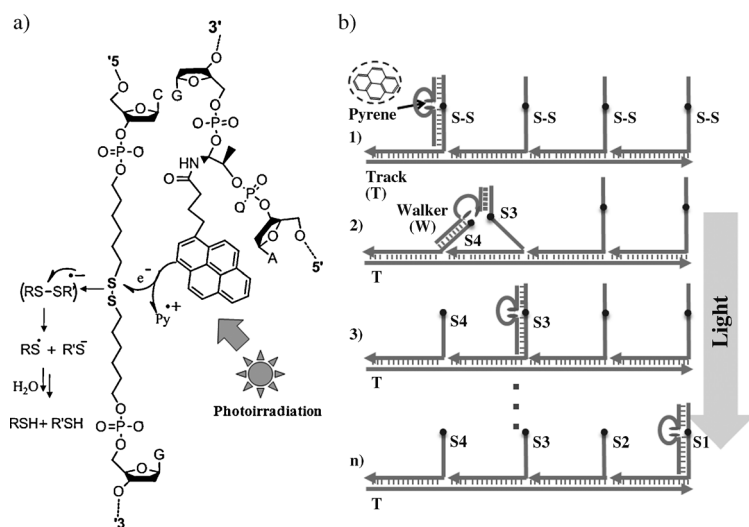


Figure 1. Photolysis and DNA walker system. a) Pyrene-assisted photolysis of disulfide within DNA structures. b) The walking principle: walker, four anchorage sites, and track form the walking system through self-assembly. When the walker takes a step, the light-triggered photolysis of the anchorage sites provides the energy for locomotion.

anchorage sites. Through specific base pairing, the track organizes the four anchorage sites into one self-assembled construction, with four walker (W) binding sites extending from the track. After the assembly, the distance between two adjacent anchorage sites corresponds to two helical pitches, roughly 7 nm. It is worth mentioning that, the sequence design of the walking system is not limited to this established one, and we just employ it for demonstration of the light-controlled motion.

The DNA walker contains two motion legs, a short leg (7 nt; nt = units of nucleotides) and a long leg (16 nt), and they are linked by a pyrene moiety that works as a photosensitizer and is incorporated into a DNA oligomer. The two motion legs are designed to respectively bind the two extender segments, which are connected by a weak disulfide bond. The recognition event between legs and anchorage sites brings the pyrene and disulfide moieties together. Irradiation at 350 nm causes pyrene-facilitated photolysis of the disulfide bond with the sufficiency required to initiate movement. Once the disulfide bond is cleaved, the shorter leg dissociates to search its surroundings for the next accessible anchorage site, while the longer leg remains bound to the extender segment, thus preventing the walker from leaving the track. Based on the toehold-mediated strand displacement,^[5] the longer leg will further move onto the anchorage site that the shorter leg binding with, finally complete one step forward. The construction of the overall walking system was verified by native polyacrylamide gel electrophoresis (N-PAGE, see Figure S1 in the Supporting Information).

In the nanosized world, random Brownian motion is much more important than gravity and momentum, which govern movement in the macroscopic world. To overcome random motion, a “Burnt Bridge” mechanism^[11] was incorporated to make the revisiting of the same anchorage site less probable. That is, by consuming the anchorage site after stepping, forward motion results in higher thermostability and statis-

tical probability compared with the backward motion (revisiting the cleaved site), provides the basis for the directional movement. In our design, this is achieved by the light-energy-powered photolysis of the anchorage extenders.

Light-powered autonomous and directional locomotion was shown by monitoring the anchorage cleavage (separation of two extender segments on opposite sides of the disulfide linker) after the DNA walker takes a step (Figure 2). Directional walking pathways, for example, **S1**→**S4** or **S4**→**S1**, were investigated. For example, from **S4** to **S1**, the walker was specifically positioned through separately prepared **T**(track)-**S1**-**S2**-**S3** and **S4**-**W**(walker) conjugates. Mixing the conjugates immediately prior to light irradiation ensured that the **S4** anchorage was the initiating site (the largest distribution binding position before irradiation) for the walker. Sequential cleavage is observed in Figure 2 by the amounts of the respective cleaved anchorage strands (shorter extender segments on one side of disulfide linker). The results are consistent with the expected direction: **S1** > **S2** > **S3** > **S4** for **S1**→**S4** and **S4** > **S3** >

S2 > **S1** for **S4**→**S1**. As a control, negligible bond cleavage was observed in the absence of the pyrene-incorporated walker (see Figure S2a in the Supporting Information). To test the integrity of this system, we synthesized another DNA track (**T***), with the anchorage sites in the order of **S3**-**S2**-**S1**-**S4**, and the gel results followed the nucleotide sequence from the track (see Figure S2b in the Supporting Information).

The progressive locomotion of the DNA walker is limited only by the spatial dimensions available to it. Specifically, after the shorter leg (7 nt) dissociates from the track, the closest anchorage site will be in the most accessible location to serve as the replacement strand. The walker will prefer the stepwise motion, instead of “hopping”, that is, after leaving **S4** site, the next step will be to the **S3**, not **S2** site. The progressive locomotion of the DNA walker was investigated using a fluorescence resonance energy transfer (FRET) assay. As the FRET donor, 6-carboxyfluorescein (6-FAM fluorophores)

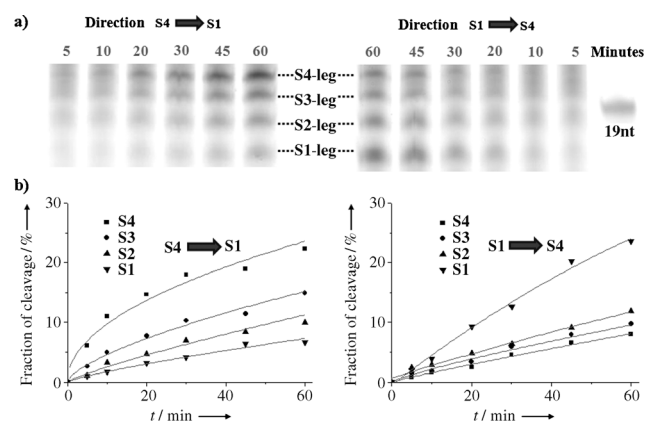


Figure 2. Directional and autonomous locomotion. a) Denatured PAGE analysis for walker movement in the **S4**→**S1** and **S1**→**S4** directions. The band shows the short cleaved substrate fragments for the respective anchorage site as a function of irradiation time. b) Quantification of the cleavage fraction using the Image J software.

were labeled on the longer leg of the walker, and Cy5, an acceptor for FAM fluorescence energy, was attached to anchorage site **S3**. Because the FRET efficiency is proportional to an inverse 6th power of the donor–acceptor distance, distance-dependent FRET is expected to occur most efficiently when the walker steps onto the **S3** site, thereby bringing FAM and Cy5 together. Indeed, consistent with our expectations, the **S1**–**S2**–**S3**–**S4** track required a longer time to reach maximal fluorescence signal than the **S4**–**S3**–**S2**–**S1** track (longer distance and more steps for progressive motion from two-step **S1**→**S3** than one-step **S4**→**S3**, see Figure S3b in the Supporting Information). Moreover, the anchorage site **S2** was labeled with another FRET acceptor, tetramethylrhodamine (TAMRA), and sequential transient FRET was shown following the progressive motion (Figure 3). In a control experiment, to further confirm such progressive movement, an **S2*** site was synthesized without a disulfide bond. Without this cleavage point to keep the walker moving, a much longer residence time on **S2*** was observed (see Figure S3c in the Supporting Information). These experiments confirmed the directionality and progressive motion of our light-powered walker.

The major merit of light-regulated DNA walker is its precise controllability, which is essential for nanosized devices. In contrast to DNA walkers fueled by DNA^[2a,5] or ATP hydrolysis,^[6] light energy can be transmitted to the system without physical contact. As a result, the initiation and termination of walking activities can be simply and immediately achieved through on/off switching of the light power source. Additionally, the motional velocity of the walker can be controlled by the intensity of the light source. As shown in Figure 4a, the motion of the DNA walker was accelerated by increasing the light intensity. Control of the locomotion speed was also investigated using a bulk fluorescence assay. Based on the FRET measurement after 350 nm irradiation with varied light power, more rapid movement was observed with increasing light intensity (see Figure S4 in the Supporting Information).

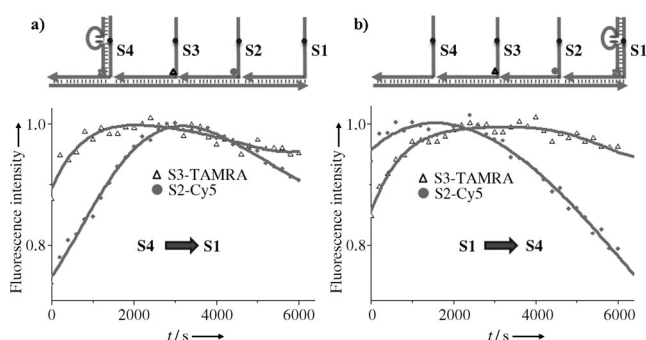


Figure 3. Progressive walking shown by FRET assay. FAM (donor fluorophore, star) labelled walker moves on the anchorage site labelled by FRET acceptor fluorophore TAMRA (triangle) and Cy5 (circle). Fluorescence intensity (662 nm for Cy5, 575 nm for TAMRA, λ_{ex} = 488 nm) was monitored during a) **S4**→**S1** and b) **S1**→**S4** tracks. The light source was obtained using the fluorometer, with light power of $66 \mu\text{Wcm}^{-2}$ at 350 nm (spectral bandwidth = 10 nm, interval time = 0.1 s).

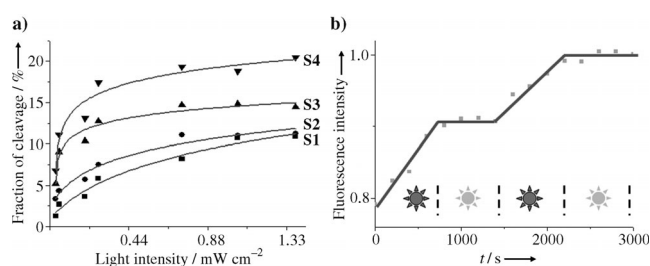


Figure 4. Controllable locomotion. a) Walking speed controlled by different irradiation power. The cleavage fraction of the respective anchorage site (along **S4**→**S1** direction) was analyzed after 45 min of irradiation at 350 nm. b) The stop and restart actions of the DNA walker are controlled by light irradiation. Monitoring the Cy5 (**S2** anchorage site) fluorescence intensity (662 nm, λ_{ex} = 488 nm) while alternating the irradiation on/off (using the light source in the fluorometer at 350 nm, light power $66 \mu\text{Wcm}^{-2}$). The walker moves along anchorage **S1**–**S2**–**S3**–**S4** on track **T**.

An inherent hindrance of chemically modulated nano-machines is the difficulty in controlling their stop and restart actions by the addition or removal of chemicals. However, this problem is easily overcome by the light-powered walking system. Figure 4b shows that the miniature walker can be regulated by simply switching the irradiation light on or off. Such controllable autonomous movement will be a significant improvement for regulating and optimizing nanorobot devices, making them potentially useful for cargo transport and other tasks.

Other properties of this light-powered nanowalker system include broad choices in design and operation. First, there is freedom in DNA sequence design. As mentioned above, the walker is comprised of three parts: two legs and one body. Irrespective of the catalytic efficiency, each of these parts can be freely modified to optimize the motion. For example, the length of the body sequence, which connects the two pyrene moieties, can be readily modified to optimize the spatial dimension available to the walker and the motional style.^[12] As a demonstration, two additional light-sensitive walkers, **W_S** and **W_L**, were synthesized with different body lengths. Both probes showed programmable walking along the track, but with different motional speeds (see Figure S5 in the Supporting Information). Elongating the body does allow faster motion, but with increased risk of more “hopping” (more than one-sized step) than “stepping” (because of increased spatial dimensions available to it, which disturb the progressive locomotion). Therefore, a compromise between speed and “hopping” could be struck for different applications. For example, in walker-based synthesis,^[2f] product purity and reaction efficiency may be more important than time requirements, thereby making the DNA walker with shorter linker length more desirable. Other operational freedoms exist with respect to physical conditions, for example, temperature and solution components. Unlike enzyme or DNAzyme-based walkers,^[5,6] which normally function at physiological temperature or certain cofactor concentration (e.g., Mg^{2+} ions), the light-powered walker can theoretically be operated under broader physical conditions (as long as the DNA strands still bind together), thus

enhancing the potential application area of the walking device.

In conclusion, we showed in this work the feasibility of designing an autonomous, but controllable, DNA walking device by incorporating photosensitive moieties within DNzyme analogue structures. Compared with “molecular motors” in nature, such light-powered walkers are still not as fast and powerful (the fraction of walkers that reach the end of track is still lower than 40%, which might be due to the equilibrium between the two disulfide molecular states, the oxidized form, S–S, and the reduced form, –SH). However, as a new type of energy supply for powering nanosized robots, the photon energy has the benefits of precise controllability and optimization freedom, while preserving autonomous, progressive motion. Considering the continuous effort to identify clean and renewable energy sources, more rationally designed light-energy-powered miniature mechanical devices will arise, emulating nature’s stepping rate for performing various tasks, for example, transferring cargoes and stimulating macroscopic motion.

Experimental Section

Denatured PAGE analysis: The denatured PAGE gels were run in 15% acrylamide (containing 19/1 acrylamide/bisacrylamide and 8.3 M urea), at 200 V constant voltage for 1.5 h using 1 × tris-borate-EDTA (TBE) as the separation buffer; normally 1.0 μM DNA strands (10 μL) are loaded for each well. The fluorescence images of gels were recorded by FAM fluorescence, with excitation at 488 nm and emission at 526 nm, using a Typhoon 9410 variable mode imager (GE Healthcare, Piscataway, NJ). The band intensities were analyzed with Image J software from NIH. Origin 8.0 was used for data analysis.

Native PAGE analysis: The binding and three-dimensional structures of the DNA walking system were observed using native PAGE gel. Normally the gel was run in 8–10% acrylamide (containing 19/1 acrylamide/bisacrylamide) solution with 1 × TBE/15 mM Mg²⁺ buffer, at 100 V constant voltage for 1 h (4°C). After that, the gel was stained 30 min using Stains-All (Sigma-Aldrich) to image the position of DNA. Photographic images were obtained under visible light with a digital camera.

FRET measurements: A FluoroMax-4 spectrofluorometer with a temperature controller (Jobin Yvon) was used for all steady-state fluorescence measurements. The locomotion of walker along the track was realized by excitation at 350 nm using the spectrofluorometer source (spectral bandwidth = 10 nm; interval time = 0.1 s). After a series of irradiation time periods, fluorescence intensities at 515 nm (FAM), 575 nm (TAMRA) and 662 nm (Cy5) were recorded using an excitation wavelength of 488 nm.

Manipulation of the walking system: The oligonucleotides employed are listed in Tables S1 and S2 in the Supporting Information. Using S4→S1 as an example, the formation of the walking system was as follows. After separate annealing (95°C–10°C, over 20 min) in 20 mM Tris buffer (pH 7.5, containing 100 mM NaCl and 10 mM MgCl₂), T-S1-S2-S3 and S4-W conjugates were mixed with final concentration for each sequence of 1.0 μM, and the sample was irradiated with a UV-B lamp (SANKO DENKI, Japan) with a 352 nm photochemical optical filter (3 nm half bandwidth; Oriol Instruments, Stratford, CT, Newport). The irradiation power employed was measured using a power meter (Newport Corp., Irvine, CA). After a series of irradiation times, the samples were removed and subjected to denatured PAGE for analysis and imaging. The FRET experiments were performed using a FluoroMax-4 spectrofluorometer with a temperature controller (Jobin Yvon). The final 300 nm concen-

tration of each DNA strand was mixed in the 10 mM Tris buffer (pH 7.5, containing 50 mM NaCl and 5 mM MgCl₂). Locomotion of the walker along the track was realized by irradiation at 350 nm using the source in the spectrofluorometer (spectral bandwidth = 10 nm; interval time = 0.1 s; light power 66 μW cm⁻²). After a series of irradiation times, fluorescence intensities at 575 (FAM), 515 (TAMRA), and 662 nm (Cy5) were recorded using excitation at 488 nm (λ_{ex} for FAM).

Received: November 2, 2011

Published online: February 1, 2012

Keywords: autonomous movement · DNA · light control · molecular devices

- [1] M. Schliwa, G. Woehlke, *Nature* **2003**, 422, 759–765.
- [2] a) K. Lund, A. J. Manzo, N. Dabby, N. Michelotti, A. Johnson-Buck, J. Nangreave, S. Taylor, R. Pei, M. N. Stojanovic, N. G. Walter, E. Winfree, H. Yan, *Nature* **2010**, 465, 206–210; b) J. Bath, A. J. Turberfield, *Nat. Nanotechnol.* **2007**, 2, 275–284; c) M. Von Delius, D. A. Leigh, *Chem. Soc. Rev.* **2011**, 40, 3656–3676; d) Y. Krishnan, F. C. Simmel, *Angew. Chem.* **2011**, 123, 3180–3215; *Angew. Chem. Int. Ed.* **2011**, 50, 3124–3156; e) H. Gu, J. Chao, S. Xiao, N. C. Seeman, *Nature* **2010**, 465, 202–205; f) Y. He, D. R. Liu, *Nat. Nanotechnol.* **2010**, 5, 778–782.
- [3] a) M. J. Barrell, A. G. Campana, M. von Delius, E. M. Geertsema, D. A. Leigh, *Angew. Chem.* **2011**, 123, 299–304; *Angew. Chem. Int. Ed.* **2011**, 50, 285–290; b) M. Von Delius, E. M. Geertsema, D. A. Leigh, D. D. Tang, *J. Am. Chem. Soc.* **2010**, 132, 16134–16145.
- [4] a) P. Yin, H. M. T. Choi, C. R. Calvert, N. A. Pierce, *Nature* **2008**, 451, 318–322; b) T. Omabegho, R. Sha, N. C. Seeman, *Science* **2009**, 324, 67–71; c) S. J. Green, J. Bath, A. J. Tuberfield, *Phys. Rev. Lett.* **2008**, 101, 238101.
- [5] a) Y. Tian, Y. He, Y. Chen, P. Yin, C. Mao, *Angew. Chem.* **2005**, 117, 4429–4432; *Angew. Chem. Int. Ed.* **2005**, 44, 4355–4358; b) J. Bath, S. J. Green, A. J. Tuberfield, *Angew. Chem.* **2005**, 117, 4432–4435; *Angew. Chem. Int. Ed.* **2005**, 44, 4358–4361; c) S. F. J. Wickham, M. Endo, Y. Katsuda, K. Hidaka, J. Bath, H. Sugiyama, A. J. Tuberfield, *Nat. Nanotechnol.* **2011**, 6, 166–169; d) R. Pei, S. K. Taylor, D. Stefanovic, S. Rudchenko, T. E. Mitchell, M. N. Stojanovic, *J. Am. Chem. Soc.* **2006**, 128, 12693–12699.
- [6] P. Yin, H. Yan, X. G. Daniell, A. J. Tuberfield, J. H. Reif, *Angew. Chem.* **2004**, 116, 5014–5019; *Angew. Chem. Int. Ed.* **2004**, 43, 4906–4911.
- [7] a) J. Shin, N. A. Pierce, *J. Am. Chem. Soc.* **2004**, 126, 10834–10835; b) W. B. Sherman, N. C. Seeman, *Nano. Lett.* **2004**, 4, 1203–1207; c) Z. Wang, J. Elbaz, I. Willner, *Nano Lett.* **2011**, 11, 304–309.
- [8] a) P. Gorostiza, E. Y. Isacoff, *Science* **2008**, 322, 395–399; b) M. Zhou, X. Liang, T. Mochizuki, H. Asanuma, *Angew. Chem.* **2010**, 122, 2213–2216; *Angew. Chem. Int. Ed.* **2010**, 49, 2167–2170; c) H. Kang, H. Liu, J. A. Phillips, Z. Cao, Y. Kim, Y. Chen, Z. Yang, J. Li, W. Tan, *Nano. Lett.* **2009**, 9, 2690–2696; d) Y. Kim, Z. Cao, W. Tan, *Proc. Natl. Acad. Sci. USA* **2008**, 105, 5664–5669.
- [9] M. You, Z. Zhu, H. Liu, B. Gulbakan, D. Han, R. Wang, K. R. Williams, W. Tan, *ACS Appl. Mater. Interfaces* **2010**, 2, 3601–3605.
- [10] a) R. Kopelman, W. Tan, *Science* **1993**, 262, 1382–1384; b) W. Tan, Z. Shi, S. Smith, D. Birnbaum, R. Kopelman, *Science* **1992**, 258, 778–781.
- [11] a) J. Mai, I. M. Sokolov, A. Blumen, *Phys. Rev. E* **2001**, 64, 011102; b) S. Saffarian, I. E. Collier, B. L. Marmer, E. L. Elson, G. Goldberg, *Science* **2004**, 306, 108–111.
- [12] Z. Wang, *Proc. Natl. Acad. Sci. USA* **2007**, 104, 17921–17926.